

**CHARACTERIZATION OF MACROSCOPIC EROSION OF
CASTELLATED AND FLAT TUNGSTEN SURFACES UNDER
ITER-LIKE TRANSIENT PLASMA LOADS**

*M.O. Myroshnyk^{1,2}, S.S. Herashchenko¹, V.A. Makhlai^{1,2}, I.E. Garkusha^{1,2}, N.N. Aksenov¹,
O.V. Byrka¹, V.V. Chebotarev¹, N.V. Kulik¹, S.I. Lebedev¹, P.B. Shevchuk¹, V.V. Staltsov¹*

¹*National Science Center “Kharkov Institute of Physics and Technology”,
Institute of Plasma Physics, Kharkiv, Ukraine;*

²*V.N. Karazin Kharkiv National University, Kharkiv, Ukraine*

E-mail: gerashchenko@kipt.kharkov.ua

The damages of tungsten targets with different geometries under repetitive transient hydrogen plasma loads have been studied with a quasi-stationary plasma accelerator QSPA Kh-50. The results of the experiments on target with geometry close to ITER divertor reference design have been compared to results of previous experiments on flat target. The plasma stream parameters were relevant to ITER ELMs (surface heat load above the melting (0.6 MJ/m^2) and below the evaporation (1.1 MJ/m^2) thresholds of tungsten and pulse duration of 0.25 ms). Surface erosion and dynamics of erosion products have been investigated in the course of repetitive plasma pulses. The crack networks and progressive corrugation occurred on the surface of all the targets exposed to a large number of plasma pulses. Melt motion leads to grow of protuberances on edges of castellated target units. Unlike the flat targets, the separation of liquid/solid particles from the edges of the units is the most significant source of the castellated targets erosion.

PACS: 52.40.HF

INTRODUCTION

At present day, tungsten is a leading candidate material for plasma facing components (PFCs) for most loaded areas in fusion reactor. Tungsten has low sputtering yield, high melting temperature and high thermal conductivity. Stationary heat loads up to 10 MW/m^2 and short duration ($<10 \text{ ms}$) transient heat loads up to 20 MW/m^2 are expected in Deuterium-Tritium phase of the experimental tokamak ITER [1]. During normal operation of tokamak in H-regime so-called ELMs (Edge localization mode) are expected. The strongest ELMs (unmitigated type I) are supposed to have the energy density up to several MJ/m^2 during 0.1–1 ms at 1...2 Hz frequencies. Transient off-normal events such as vertical displacement events (VDEs, 60 MJ/m^2 in 100...300 ms) and the thermal quench of disruptions (30 MJ/m^2 in 1...10 ms), will cause extreme heat loads to PFCs [2]. Transient heat loads produce strong surface damage (cracking and melting) of tungsten, which significantly affects lifetime and performance of tungsten PFCs. Therefore, comprehensive investigations of the heat/particle loads influence on PFCs in conditions relevant to fusion reactor are required.

Castellated geometry is approved as a reference design for ITER divertor plates [3]. Such sectioning of the surface of PFCs is to be used in order to reduce the influence of electric currents induced on the metallic surfaces during the reactor operation as well as to minimize the thermal stresses and resulting tungsten erosion, which caused by the formation of macro-crack meshes on the surface [4]. Nevertheless it is expected that sharp edges in the castellated geometry of the ITER divertor structure may be additional source of enhanced

erosion, i.e., the emission of liquid/solid particles into the plasma region [5]. Presence of a liquid layer of molten material could further results in splashing of droplets under the influence of different external forces, such as gradients of both plasma pressure and recoil pressure of evaporating material, as well as surface tension, Lorentz forces, and melt instabilities [6-13].

This paper presents a comparison of surface damages, erosion and dynamics of liquid/solid particle ejection for planar and castellated tungsten targets under the QSPA Kh-50 plasma exposures simulating ITER ELMs.

**1. EXPERIMENTAL DEVICE,
DIAGNOSTICS AND TARGET DESIGN**

Experimental simulations of ITER transient events with relevant heat load parameters (energy density and the pulse duration) as well as particle loads were carried out with a quasi-stationary plasma accelerator QSPA Kh-50 [5-14]. Targets with two different constructions were used in the experiments. Targets have been manufactured from sintered tungsten sample of Plansee AG trademark with sizes $5 \times 5 \times 1 \text{ cm}$. Flat target was covered by a molybdenum diaphragm with a hole of 3 cm to protect the target edges from the plasma impact [5, 9]. For another target, slits were cut on the target's surface to obtain castellated geometry in accordance with ITER divertor reference design [15] (Fig. 1), with the size of each castellated element of $24 \times 12 \times 5 \text{ mm}$ and the width of gaps between elements of 1 mm.

The main parameters of QSPA Kh-50 plasma streams were as follows: ion impact energy was about 0.4 keV, the maximum plasma pressure up to 0.32 MPa

ISSN 1562-6016. BAHT. 2019. №1(119)

(that is larger than plasma pressure expected in ITER (up to 0.01 MPa), and the stream diameter of 18 cm. The plasma pulse shape was approximately triangular, and the pulse duration of 0.25 ms [8, 11-14].

The flat and castellated tungsten targets were irradiated by plasma streams with a surface heat load reproducing unmitigated ITER ELMs Type I i.e. above the melting (0.6 MJ/m^2) and below the evaporation (1.1 MJ/m^2) thresholds of tungsten [8, 12]. The surface of the target was placed perpendicularly to the plasma stream direction. The target before each irradiating pulse was kept at room temperature.

The energy density in impacting plasma stream and surface heat loads were measured by the local calorimeters. The plasma pressure was measured by piezoelectric detectors. Observations of plasma interactions with exposed surfaces (see Fig. 1), the dust particle dynamics and the droplets monitoring were performed with a high-speed 10 bit CMOS pco.1200 s digital camera PCO AG (exposure time from $1 \mu\text{s}$ to 1 s, spatial resolution $12 \times 12 \text{ m}$ and within the spectral range from 290 to 1100 nm).

Surface analysis of exposed samples was carried out with an optical microscope MMR-4, equipped with CCD camera.

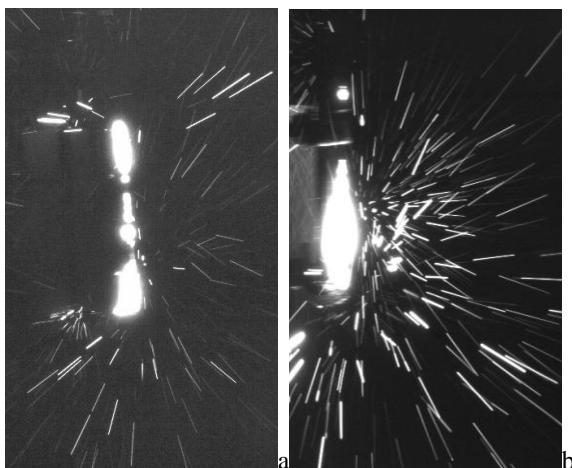


Fig. 1. Images of droplet traces after small number of plasma exposes of castellated (a) and flat (b) targets
Better to indicate number of pulse

2. EXPERIMENTAL RESULTS

2.1. STUDIES OF LIQUID/SOLID PARTICLES EJECTION

Pronounced particle ejection was observed during the plasma-surface interaction (see Fig. 1). The quantity of the particles ejected from the surface varies from pulse to pulse. For castellated target, continuous decrease of number of ejected particles was observed with increase of plasma pulses [15]. Number of ejected particles is essentially less after hundred plasma pulses. In the case of flat target irradiation, mass loss rate also changes with increase of pulse number. After 100 pulses the mass loss reached $3 \mu\text{g} \cdot \text{cm}^{-2}$ per pulse and increased up to $5 \mu\text{g} \cdot \text{cm}^{-2}$ per pulse for the next 100 pulses [13].

The dependence of ejected particles` velocity distribution from the start-up time from the exposed surface was revealed from the analysis of camera

frames. Values of velocities of ejected particles are found to be similar to the typical velocities of particles registered in earlier experiments [11-13, 15]. The particles start time from the surface is in range of 0...1.4 ms ($t=0$ corresponds to the beginning of plasma-target interaction). The maximum velocity of ejected particles achieved 25 m/s for both castellated and flat targets [11, 15].

2.2. THE EROSION FEATURES OF THE TARGET'S SURFACE

Either castellated or flat tungsten target`s surface was significantly damaged after large number of plasma pulses. Cracks networks and re-solidified layer developed on the surfaces` in the course of plasma irradiation (Fig. 2). Edges of the castellated target units demonstrate higher erosion/damaging rates compared to flat target`s surface. At some locations, erosion of millimeter-scale chunks of material has been observed on castellated target edges.

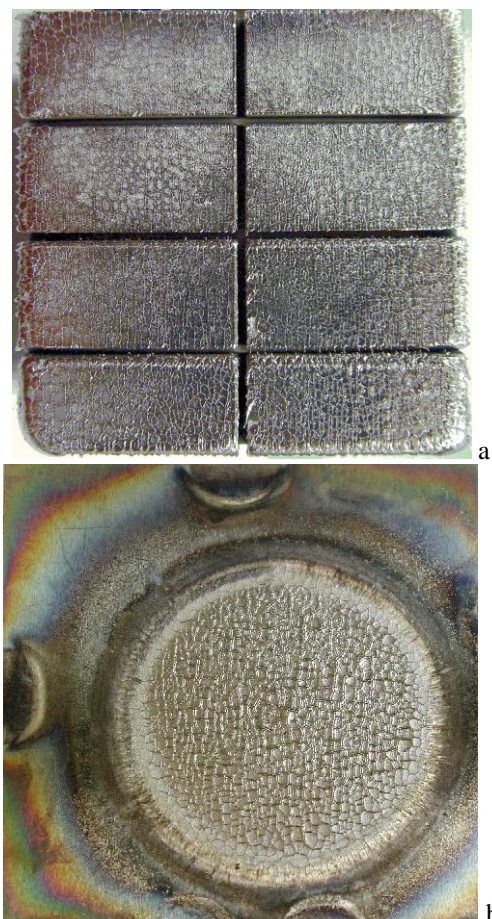


Fig. 2. General view of a castellated (a) and flat (b) tungsten target exposed to 200 plasma pulses

Major crack networks appear on all targets` surfaces after plasma pulses. An average cell size of major crack networks is up to $500 \mu\text{m}$ (Fig. 3). It was shown in previous experiments that mean unit size of the major cracks mesh does not depend on the tungsten grade. This mesh is attributed to the ductile-to-brittle transition effects and elastic energy stored in the stressed tungsten surface layer [8, 10]. Re-solidification of the molten layer causes the micro-crack networks development

against the background of major crack mesh. The micro-crack network has a cell size of about 10...50 μm . The width of micro-cracks does not exceed 1 μm . They appear after the melt thickness exceeds 5...10 μm . The melt motion also causes the partial filling of macro-cracks [10-12]. Evolution of fine cracks become very important for the surface erosion changes after several hundreds of pulses. A large number of plasma impacts with heat loads above the melting threshold causes the progressive corrugation inside each surface cell in between of fine cracks and also pits and submicron structures on surfaces of both targets [10, 11, 19].

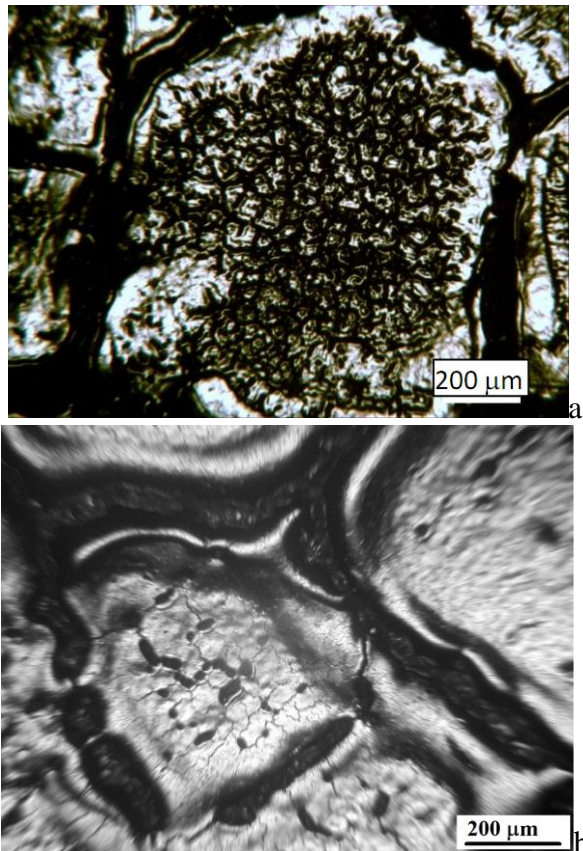


Fig. 3. Images of castellated (a) and flat (b) tungsten target's surface after exposure to 200 QSPA plasma pulses

The droplet splashing and dust ejection during the plasma-surface interaction may occur due to the development of Kelvin-Helmholtz or Rayleigh-Taylor instabilities [16, 17] and separation of particles from the crack edges. The most overheated parts of castellated target are edges of the units. Therefore, they are melted earlier in comparison to the surface. The melt motion and its solidification lead to appearance of pronounced protuberances on the edges of castellated units [15, 18]. The largest protuberances are observed on the outer edge of target, which is the most overheated part of the target (Fig. 4). Appearance of protuberances on the edges of the units leads to their further separation during following plasma impacts. Protuberances appear after first few plasma pulses then they constantly grow and break away from target during applied cycle of plasma pulses. Edges of units are substantial source of large – size liquid and solid particles, which ejected from the

castellated target. In comparison, average size of emitted particles from flat targets is essentially smaller due to absence of edges.

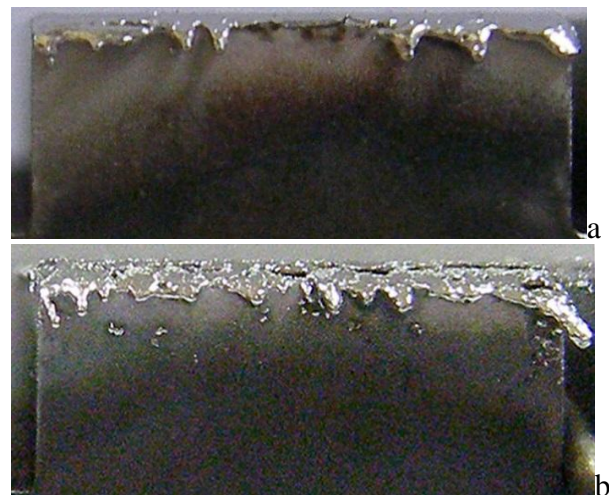


Fig. 4. Images of castellated target's edge after 20 (a), and 200 (b) plasma pulses

CONCLUSIONS

Comparative studies of erosion features and surface morphology for flat tungsten target and that for castellated target geometry (similar to ITER reference design) have been performed with quasi-stationary plasma accelerator QSPA Kh-50. The applied repetitive plasma loads were above the melting, but below the evaporation thresholds of tungsten.

Significant erosion and damage of target's surfaces is observed after plasma heat loads. Plasma impacts resulted in ejection of liquid/solid tungsten particles from the irradiated surfaces. For castellated target, the number of ejected particles and their velocities strongly depends on the number of plasma pulses performed. As the pulse number increases, the amount of particles separated from target became smaller and their velocity decreases. Flat target's mass loss rate also depended on number of plasma pulses.

For both targets, macro-crack networks and micro-crack meshes inside the macro-crack networks appeared on exposed surfaces. Micro-cracks are filled during melt stage and appear again after the re-solidification.

Castellated structure leads to growing protuberances on the edges of target units and their separation during following plasma pulses.

For castellated targets, erosion of unit edges substantially exceeds the erosion of central surface areas. Unit edges are primary source of separated liquid/solid particles, which is not typical for flat targets.

ACKNOWLEDGEMENTS

This work has been also supported by National Academy Science of Ukraine project X-4-3/2018, NMRT-2/2018, II-5/24-2018 and IAEA's CRP F43022. This work has been carried out within the framework of the EUROfusion Consortium and has received funding from the Euratom research and training programme 2014-2018 under grant agreement № 633053.

The views and opinions expressed herein do not necessarily reflect those of the European Commission. Work performed under EUROfusion WP PFC.

This work has also been supported by National Academy Science of Ukraine project X-4-3/2018, NMRT-2/2018, П-5/24-2018 and IAEA's CRP F43022.

REFERENCES

1. Y. Ueda et al. // *Nucl. Fusion*. 2017, v. 57, p. 092006.
2. H. Bolt et al. // *Journal of Nuclear Materials*. 2002, v. 307-311, p. 43.
3. Ch. Linsmeier et al. // *Nucl. Fusion*. 2017, v. 57, p. 092012.
4. T. Hirai et al. // *Phys. Scr.* 2014, v. T159, p. 014006.
5. M. Komm et al. // *Plasma Phys. Control. Fusion*. 2011, v. 53, p. 115004.
6. B.N. Bazylev et al. // *Fusion Engineering and Design*. 2005, v. 75-79, p. 407.
7. G. Miloshevsky, A. Hassanein // *Nucl. Fusion*. 2014, v. 54, p. 043016.
8. I.E. Garkusha et al. // *Journal of Nuclear Materials*. 2005, v. 337-339, p. 707-711.
9. I.E. Garkusha et al. // *Journal of Nuclear Materials*. 2007, v. 363-365, p. 1021-1025.
10. I.E. Garkusha et al. // *Journal of Nuclear Materials*. 2009, v. 386-388, p. 127.
11. I.E. Garkusha et al. // *Fusion Sci. Technol.* 2014, v. 65(2), p. 186.
12. V.A. Makhraj et al. // *Phys. Scr.* 2014, v. T159, p. 014024.
13. S. Pestchanyi et al. // *Phys. Scr.* 2011, v. T145, p. 014062.
14. I.E. Garkusha et al. // *Phys. Scr.* 2016, v. 91, p. 094001.
15. S.S. Herashchenko et al. // *Problems of Atomic Science and Technology. Ser. "Plasma Physics"*. 2017, № 1, p. 119-122.
16. G.V. Miloshevsky, A. Hassanein, et al. // *Nucl. Fusion*. 2010, v. 50, p. 115005.
17. B. Bazylev et al. // *Fusion Engineering and Design*. 2008, v. 83, p. 1077-1081.
18. S.S. Herashchenko et al. // *Problems of Atomic Science and Technology. Ser. "Plasma Physics"*. 2014, № 6 (94), p. 44.
19. A.A. Shoshin, A.V. Arzhannikov, A.V. Burdakov, et al. // *Fusion Science and Technology*. 2011, v. 59 (1T), p. 57-60

Article received 15.01.2019

ХАРАКТЕРИСТИКА МАКРОСКОПИЧЕСКОЙ ЭРОЗИИ ПОВЕРХНОСТЕЙ ЗУБЧАТЫХ И ПЛОСКИХ МИШЕНЕЙ В УСЛОВИЯХ ПЕРЕХОДНЫХ ПЛАЗМЕННЫХ НАГРУЗОК В ИТЭР

М.О. Мирошник, С.С. Геращенко, В.А. Махлай, И.Е. Гаркуша, Н.Н. Аксенов, О.В. Бырка, В.В. Чеботарев, Н.В. Кулик, С.И. Лебедев, П.Б. Шевчук, В.В. Стальцов

Изучены повреждения вольфрамовых мишеней с различной геометрией при повторяющихся импульсных нагрузках водородной плазмой в квазистационарном плазменном ускорителе КСПУ X-50. Результаты экспериментов с мишенью, имеющей близкую к конструкции дивертора ИТЭР геометрию, сопоставлены с результатами для плоских мишеней. Параметры потоков плазмы выбраны близкими к ELM в ИТЭР (поверхностная тепловая нагрузка выше порога плавления ($0,6 \text{ МДж/м}^2$) и ниже порога испарения вольфрама ($1,1 \text{ МДж/м}^2$), длительность импульса $0,25 \text{ мс}$). Представлена характеристика эрозии поверхностей и эжекции частиц с мишеней в условиях повторяющихся плазменных импульсов. На поверхностях мишеней, облученных большим количеством плазменных импульсов, обнаружены сетки трещин и выраженная волнистая структура. Движение расплава приводит к росту выступов на краях элементов зубчатой мишени. В отличие от плоских мишеней отделение жидких/твердых частиц с краев элементов составляет наиболее существенный источник эрозии зубчатых мишеней.

ХАРАКТЕРИСТИКА МАКРОСКОПІЧНОЇ ЕРОЗІЇ ПОВЕРХОНЬ ЗУБЧАТИХ І ПЛАСКИХ МІШЕНЕЙ В УМОВАХ ПЕРЕХІДНИХ ПЛАЗМОВИХ НАВАНТАЖЕНЬ В ІТЕР

М.О. Мирошник, С.С. Геращенко, В.О. Махлай, І.Є. Гаркуша, М.М. Аксьонов, О.В. Бирка, В.В. Чеботарьов, М.В. Кулик, С.І. Лебедев, П.Б. Шевчук, В.В. Стальцов

Вивчено пошкодження вольфрамових мишеней з різною геометрією при повторюваних імпульсних навантаженнях водневої плазмою в квазістаціонарному плазмовому прискорювачі КСПП X-50. Результати експериментів з мішенню, що має геометрію близьку до конструкції дивертора ІТЕР, зіставлені з результатами для плоских мишеней. Параметри потоків плазми обрані близькими до ELM в ІТЕР (поверхнєве теплове навантаження вище порога плавлення ($0,6 \text{ МДж/м}^2$) та нижче порога випаровування вольфраму ($1,1 \text{ МДж/м}^2$), тривалість імпульсу $0,25 \text{ мс}$). Представлена характеристика ерозии поверхонь і ежекції частинок з мишеней в умовах повторюваних плазмових імпульсів. На поверхнях мишеней, опромінених великою кількістю плазмових імпульсів, виявлені сітки тріщин і виражена хвиляста структура. Рух розплаву призводить до зростання виступів на краях елементів зубчатої мишени. На відміну від плоских мишеней відділення рідких/твердих частинок з країв елементів становить найбільш істотне джерело ерозии зубчастих мишеней.